doi:10.1093/brain/awv155 BRAIN 2015: 138; 2347–2358 | 2347

BRAIN
A JOURNAL OF NEUROLOGY

Heterozygous *HTRA1* mutations are associated with autosomal dominant cerebral small vessel disease

Edgard Verdura,[1,2] Dominique Hervé,[1,2,3,*] Eva Scharrer,[4,*] Maria del Mar Amador,[5] Lucie Guyant-Maréchal,[6] Anne Philippi,[1,2] Astrid Corlobé,[7] Françoise Bergametti,[1,2] Steven Gazal,[8] Carol Prieto-Morin,[1,2,5] Nathalie Beaufort,[4] Benoit Le Bail,[9] Irina Viakhireva,[10] Martin Dichgans,[4,11] Hugues Chabriat,[1,2,3] Christof Haffner[4] and Elisabeth Tournier-Lasserve[1,2,5]

*These authors contributed equally to this work.

Cerebral small vessel disease represents a heterogeneous group of disorders leading to stroke and cognitive impairment. While most small vessel diseases appear sporadic and related to age and hypertension, several early-onset monogenic forms have also been reported. However, only a minority of patients with familial small vessel disease carry mutations in one of known small vessel disease genes. We used whole exome sequencing to identify candidate genes in an autosomal dominant small vessel disease family in which known small vessel disease genes had been excluded, and subsequently screened all candidate genes in 201 unrelated probands with a familial small vessel disease of unknown aetiology, using high throughput multiplex polymerase chain reaction and next generation sequencing. A heterozygous *HTRA1* variant (R166L), absent from 1000 Genomes and Exome Variant Server databases and predicted to be deleterious by *in silico* tools, was identified in all affected members of the index family. Ten probands of 201 additional unrelated and affected probands (4.97%) harboured a heterozygous *HTRA1* mutation predicted to be damaging. There was a highly significant difference in the number of likely deleterious variants in cases compared to controls ($P = 4.2 \times 10^{-6}$; odds ratio = 15.4; 95% confidence interval = 4.9–45.5), strongly suggesting causality. Seven of these variants were located within or close to the HTRA1 protease domain, three were in the N-terminal domain of unknown function and one in the C-terminal PDZ domain. *In vitro* activity analysis of *HTRA1* mutants demonstrated a loss of function effect. Clinical features of this autosomal dominant small vessel disease differ from those of CARASIL and CADASIL by a later age of onset and the absence of the typical extraneurological features of CARASIL. They are similar to those of sporadic small vessel disease, except for their familial nature. Our data demonstrate that heterozygous *HTRA1* mutations are an important cause of familial small vessel disease, and that screening of *HTRA1* should be considered in all patients with a hereditary small vessel disease of unknown aetiology.

1 INSERM UMR 1161, Génétique et Physiopathologie des Maladies Cérébro-vasculaires, Paris, France
2 Université Paris Diderot, Sorbonne Paris Cité, UMR-S1161, Paris, France
3 AP-HP, Groupe Hospitalier Saint-Louis Lariboisière-Fernand-Widal, Service de Neurologie, Centre de Référence des Maladies Vasculaires Rares du Cerveau et de l'Oeil (CERVCO), Paris, France
4 Institute for Stroke and Dementia Research, Klinikum der Universität München, Ludwig Maximilians University, Munich, Germany
5 AP-HP, Groupe Hospitalier Saint-Louis Lariboisière-Fernand-Widal, Service de Génétique Moléculaire Neurovasculaire, Centre de Référence des Maladies Vasculaires Rares du Cerveau et de l'Oeil (CERVCO), Paris, France
6 Service de Neurophysiologie, Hôpital Charles Nicolle, Rouen, France
7 Service de Neurologie, Hôpital Gui de Chauliac, Montpellier, France

Received January 17, 2015. Revised March 13, 2015. Accepted April 14, 2015. Advance Access publication June 10, 2015

8 Plateforme de Génomique Constitutionnelle du GHU Nord, Assistance Publique des Hôpitaux de Paris (APHP), Hôpital Bichat, Paris, France
9 Service de Neurologie, CH Bretagne Sud, Lorient, France
10 Service de Neurologie, Hôpital de la Cavale Blanche, Brest, France
11 Munich Cluster for Systems Neurology (SyNergy), Munich, Germany

Correspondence to: Pr. Elisabeth Tournier-Lasserve,
INSERM UMR 1161,
Faculté de Médecine Paris Diderot (site Villemin),
10 avenue de Verdun,
75010 Paris, France
E-mail: tournier-lasserve@univ-paris-diderot.fr

Keywords: small vessel disease; vascular dementia; *HTRA1*; CARASIL; CADASIL

Abbreviations: CADASIL = cerebral autosomal dominant arteriopathy with subcortical infarcts and leukoencephalopathy; CARASIL = cerebral autosomal recessive arteriopathy with subcortical infarcts and leukoencephalopathy; SVD = small vessel disease

Introduction

Cerebral small vessel disease (SVD) is a heterogeneous group of disorders affecting small arteries, arterioles, veins, and/or capillaries of the brain (Pantoni, 2010; Wardlaw *et al.*, 2013). Their two main clinical consequences are stroke and cognitive impairment. Typical neuroimaging features include white matter lesions associated with small infarctions, microbleeds, and macrobleeds. In most cases, SVD is sporadic, with age and hypertension representing the prevailing risk factors. However, several early-onset monogenic forms of SVD have been reported in adult patients, the majority of them with a dominant inheritance pattern. They include CADASIL (cerebral autosomal dominant arteriopathy with subcortical infarcts and leukoencephalopathy), inherited cerebral amyloid angiopathies and angiopathies associated with mutations of *COL4A1* and *COL4A2* genes (Joutel *et al.*, 1996; Gould *et al.*, 2006; Revesz *et al.*, 2009). CADASIL is caused by *NOTCH3* mutations and is by far the most common hereditary SVD with more than 500 families reported and a 10–15% mutation rate in patients with SVD referred for *NOTCH3* molecular screening, the second one being *COL4A1/COL4A2* angiopathies (unpublished data) (Chabriat *et al.*, 2009). By contrast, CARASIL (cerebral autosomal recessive arteriopathy with subcortical infarcts and leukoencephalopathy) is a very rare autosomal recessive SVD caused by biallelic mutations of the *HTRA1* gene (high temperature requirement protease A1); only 12 *HTRA1* mutated CARASIL families have been reported worldwide so far (Hara *et al.*, 2009; Nozaki *et al.*, 2014). While the identification of mutated genes has provided invaluable tools for diagnosing monogenic SVD forms, molecular screening of those genes in routine diagnosis identifies the causative mutation in $<20\%$ of patients referred for a familial SVD, which strongly suggests that other genes may be involved.

Herein, we used genome-wide linkage analysis and whole exome sequencing to identify the gene involved in an autosomal dominant SVD family in which SVD genes previously known to lead to an autosomal dominant SVD were excluded. We then screened a panel of 201 unrelated patients with a familial SVD of unknown aetiology to estimate the frequency of mutations of this gene in familial SVD.

Materials and methods

Participants and study design

Two siblings and one of their first cousins (Family F1) were referred for stroke and/or cognitive impairment associated with diffuse white matter hyperintensities (genealogical tree shown in Fig. 1). Detailed clinical and neuroimaging features of these patients are presented in the 'Results' section.

A panel of 201 unrelated SVD probands referred for *NOTCH3* molecular screening in the Genetics department of Lariboisière hospital were also included in this study on the basis of the following criteria: (i) having at least one first or second degree relative with a clinical history of stroke and/or vascular dementia; and (ii) being screened negative for mutations in the 23 exons of *NOTCH3* known to be involved in CADASIL. Mean age of this cohort at referral for molecular screening was 57 years (standard deviation = 11.6). This panel was used to search for mutations in the candidate genes identified in Family F1 (see below and Supplementary material).

All patients and participating relatives provided written informed consent for participation in genetic studies, in accordance with ethical recommendations in France for genetic disorders. Informed consent forms were approved by local medical ethics comittees or CPP Ile de France (N° 0711588).

One hundred and ninety-two healthy controls of French origin were used as a control group for *HTRA1* candidate variants analysis. Additional control data were obtained from the public Exome Variant Server (EVS) database ($n = 4300$ European Americans) and 1000 Genomes database ($n = 379$ Europeans).

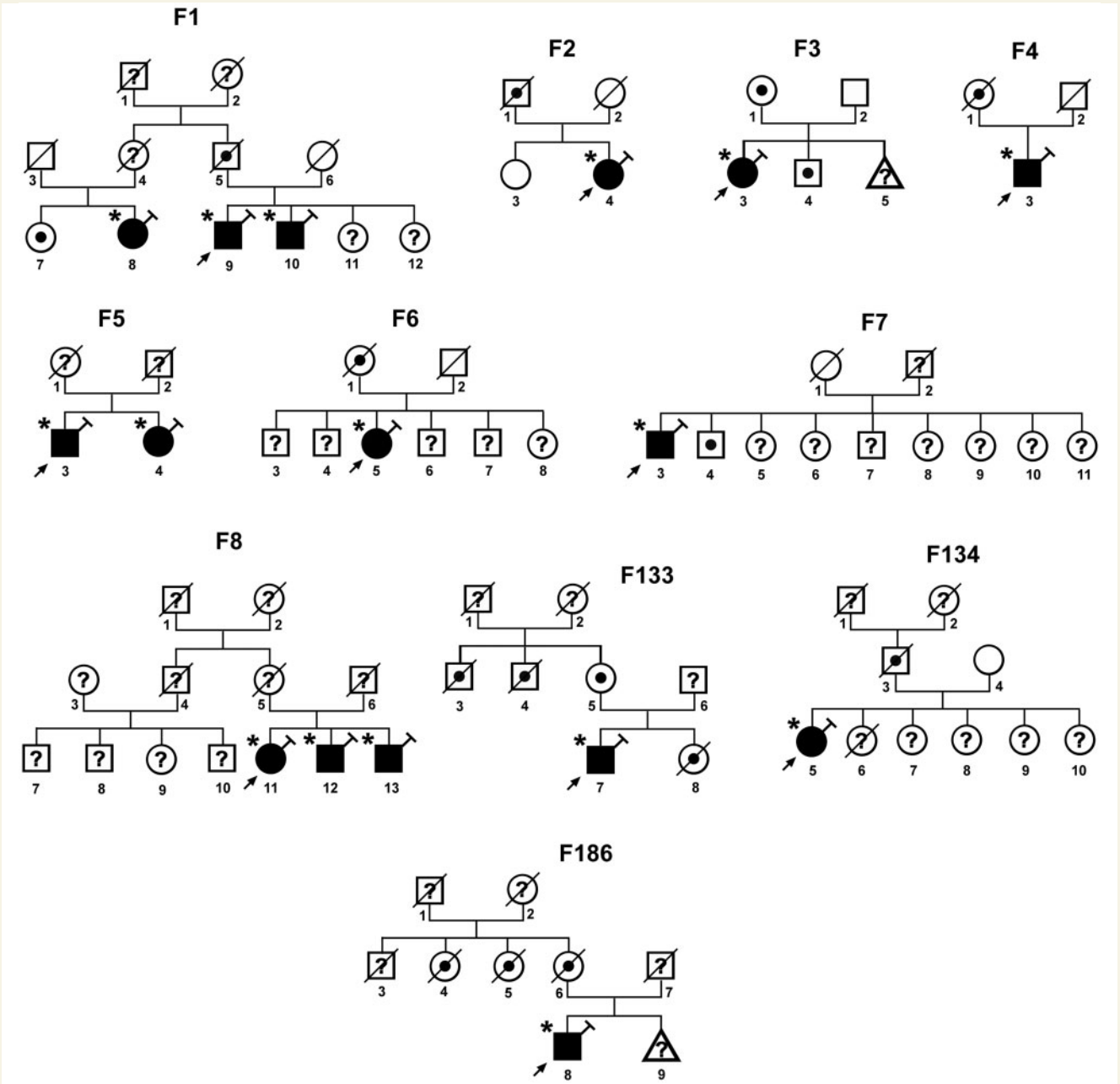

Figure 1 Genealogical trees of the 11 mutated probands. Square = male; circle = female; diagonal black line = deceased individual; black filled symbol = clinically and MRI proven affected individual; empty symbol = clinically healthy relative; black dot = affected individual based on family history and/or clinical charts; question mark = unknown status; syringe symbol = blood sampled individuall; asterisk: individual showing an *HTRA1* deleterious variant.

Procedures

Whole-genome linkage analysis was performed in Family F1 with data obtained with Affymetrix GeneChip® Human Mapping 250K arrays (Supplementary material). Parametric multipoint linkage analysis was performed with MERLIN assuming an autosomal dominant inheritance, a complete penetrance, a disease allele frequency of 0.0001, and no phenocopy. Intervals reaching the maximum theoretical LOD score achievable in this family were considered as possibly linked. Intervals with LOD scores lower than −2 and larger than 2 cM were considered as excluded for linkage.

Whole exome sequencing of the three patients of Family F1 was performed at IntegraGen platform. Variant annotation was done by an internal bioinformatics pipeline (IntegraGen). Only missense, nonsense, insertion/deletion variants or variants potentially affecting splicing were kept for further analysis. Variants present in dbSNP132, as well as those reported with a minor allele frequency >0.1% in the 1000 Genomes Project, EVS or IntegraGen exome database (96 French exomes) were excluded. Candidate variants were further selected when (i) shared by all three affected patients in a heterozygous state; and (ii) located outside regions previously excluded by genome-wide linkage analysis.

For screening of candidate genes identified in Family F1, we used Fluidigm multiplex PCR combined with next generation sequencing (191 unrelated patients; see Supplementary material) and whole exome sequencing data (10 unrelated patients for whom whole exome sequencing was also performed at IntegraGen platform).

Standard PCR amplification and Sanger sequencing were used to confirm all candidate variants detected by Illumina sequencing. When available, patients' relatives were also sequenced. In addition, Sanger sequencing of 96 DNA samples of healthy French individuals was performed to screen exons of candidate genes in which candidate variants were located. *HTRA1* exon 1 was sequenced in 192 DNA samples of healthy French individuals.

Candidate variants were analysed by three prediction programs: PolyPhen-2, SIFT, and MutationTaster. Potential splice-affecting variants were analysed by the Alamut Splicing Analysis package (Interactive Biosoftware).

Frequency of likely deleterious variants was compared between cases and two control samples from online databases: European-American controls from Exome Variant Server (EVS; $n = 4300$) and European controls from 1000 Genomes project ($n = 379$). The frequency of *HTRA1* variants in cases and controls was compared by a Fisher's exact test on a 2×2 contingency table. All the tests were two-sided, with a P-value of 0.05 considered significant and odds ratios (OR) and 95% confidence intervals (CI) were calculated. Analyses were performed using the statistical analysis package R.

Expression constructs, conditions used for transfection, collection of conditioned media, protein electrophoresis, immunoblotting and procedures used to measure the activity (Beaufort *et al.*, 2014) of the various *HTRA1* mutants are detailed in the Supplementary material.

Results

Clinical and neuroimaging features of Family F1 patients

The genealogical tree of Family F1 is shown in Fig. 1. Patient F1-9, the proband of this family, is a senior executive 69-year-old male with moderate hypercholesterolaemia but no other vascular risk factor. He had a history of sciatica related to a lumbar disk prolapse. Since age 66 he reported a progressive reduction of cognitive performances without significant impact on his daily activities and complained of gait disturbance since age 68. At age 69 he experienced an acute episode of left-sided hemiparesis that completely resolved within 8 days. His neurological examination performed at the time of MRI examination showed a subtle left-sided ataxia. His blood pressure was 134/70 mmHg. Neuropsychological testing revealed mild alterations in processing speed, executive functions, and verbal episodic and visuospatial memory performances suggestive of subcortical cognitive impairment. Mini-Mental State Examination score was 29/30. Mood was found to be mildly depressed. The standard vascular work-up (EKG, echocardiography, cervical and transcranial ultrasound examination, blood cell count, sedimentation rate, creatinine level) and fundus examination were normal.

His 64-year-old brother (Patient F1-10) had no vascular risk factor. He had a history of arthritis of small and large joints. At age 55, he presented a major depressive episode. He subsequently had cognitive complaints and decided to retire early at age 58 years. At 62 years of age, he experienced recurrent attacks of visual, sensory and aphasic migraine aura with or without headache. His neurological examination was normal. His blood pressure was at 136/78 mmHg. Cognitive testing showed alterations of performances in tests evaluating attention, executive functions and verbal episodic memory, and executive functions. Mini-Mental State Examination score was 25/30. The standard vascular work-up was normal at time of MRI examination, as well as the fundus examination. In addition, the following exams were in the normal range: 24-h blood pressure monitoring, anticardiolipid antibodies, antinuclear antibodies, anti-beta-2 GP1 antibodies, and homocysteine level.

Patient F1-8, a first cousin of Patients F1-9 and F1-10, is a 65-year-old female with a long history of well-controlled hypertension and hypercholesterolaemia. At age 60 years, she had some cognitive complaints and at 61 years, an acute episode of right hemiparesis that lasted 24 h. Her neurological examination showed mild bradykinesia, micrographia, pyramidal signs with diffuse increased reflexes. Blood pressure was 140/90 mmHg. She had a cognitive slowing, but cognitive testing including Mini-Mental State Examination, Mattis Dementia Rating Scale, Grober and Buschke Verbal Learning Test, verbal fluencies, Rey figure copy and oral naming were normal. The standard vascular work-up was normal at time of MRI examination. Complete ophthalmological examination, electrophysiological studies of the limbs and electronic microscopy skin biopsy were normal.

The father of Patients F1-9 and F1-10 had a history of dementia starting during the sixth decade of life. He died at 75 years while he was still able to walk with help. His father, died in his late seventies several days after the sudden onset of a hemiplegia. Patient F1-7, sister of Patient F1-8, presents a cognitive impairment that started after 60 years of age. Their mother died at age 70 years of unknown cause.

MRI showed in all three patients diffuse white matter hyperintensities affecting supratentorial white matter, external capsules and pons but sparing the temporal lobes (Fig. 2). Patients F1-9 and F1-8 had confluent and diffuse white matter hyperintensities in the centrum semi-ovale associated with hemispheric and pontine lacunes, while Patient F1-10 had early confluent, less diffuse white matter hyperintensities and no lacune. Patient F1-8 was the only one to show microbleeds on gradient-echo images; those numerous microbleeds were located in the deep grey nuclei and subcortical areas. All patients had multiple dilated perivascular spaces, clearly visible on T_2

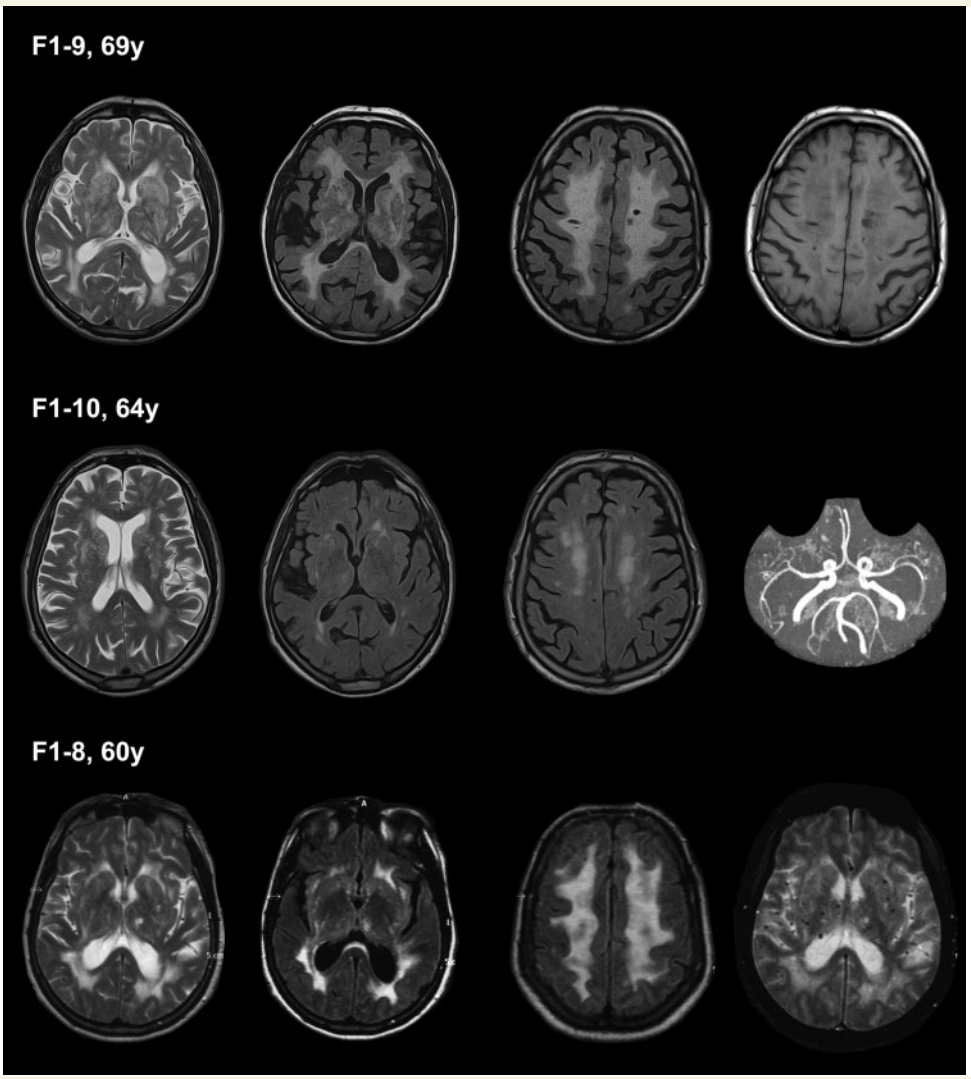

Figure 2 MRI data obtained in Patients F1-9, F1-10 and F1-8. *Left column:* T_2-weighted images. *Central columns:* FLAIR images. *Right column:* T_1-weighted image (*top*), 3D time of flight image (*middle*) and gradient-echo image (*bottom*). Extensive white matter hyperintensities in Patients F1-9 and F1-8 and less diffuse white matter hyperintensities in Patient F1-10 are detected on FLAIR images. Multiple dilated perivascular spaces corresponding to so-called *état criblé* were observed in Patients F1-9 and F1-10 on T_2-weighted images. Lacunes are found in Patients F1-9 and F1-8. Microbleeds were detected on gradient-echo images only in Patient F1-8 (juxtacortical areas and deep grey nuclei).

images and leading to so-called *état criblé* in Patients F1-9 and F1-10.

Sequence analysis of the 23 exons encoding the 34 epidermal growth factor (EGF)-like repeats in the extracellular region of the NOTCH3 receptor was negative in all patients. Screening of genomic DNA of Patient F1-8 for *APP* mutations and duplication was also negative.

Identification of candidate variants in Family F1

Genome-wide linkage analysis conducted in Family F1 excluded 79% of the genome (LOD score < -2), including all known SVD loci. We identified 28 regions reaching the theoretical maximal LOD score achievable in this family (LS = 0.903) over a minimum distance of 2 cM (Supplementary Fig. 1).

Subsequent whole exome sequencing of the three affected family members was performed. Filtering strategy and data obtained are presented in Supplementary Table 1. A total of 11 candidate variants, including six single nucleotide variants and five insertion/deletion (Indel) variants were identified. Six of 11 variants were located in regions excluded by linkage analysis and were therefore not considered. The five remaining variants were missense variants located in *HTRA1* (NM_002775.4), *TTBK2* (NM_173500.3), *C15orf43* (NM_152448.2), *CPEB1* (NM_030594.4) and *ZNF785* genes (NM_152458.6) (Supplementary Table 2). They were all absent from 1000 Genomes, EVS and IntegraGen databases, and confirmed by Sanger sequencing to cosegregate with the affected

Table 1 Rare heterozygous *HTRA1* variants identified in the familial SVD probands

Family	cDNA change	Predicted protein change	Protein domain	Intron/ Exon	PolyPhen-2[a] (HumVar)	SIFT[a]	Mutation Taster[a]	1000 Genomes frequency	EVS frequency	Sanger sequencing results
F1	c.497 G > T	p.Arg166Leu*	None	Exon 2	Probably damaging	Deleterious	Disease causing	Absence[b]	Absence	Confirmed
F2	c.517 G > C	p.Ala173Pro*	None	Exon 2	Possibly damaging	Deleterious	Disease causing	Absence	Absence	Confirmed
F3	c.852 C > A	p.Ser284Arg*	Serine protease	Exon 4	Probably damaging	Deleterious	Disease causing	Absence	Absence	Confirmed
F4	c.854 C > A	p.Pro285Gln*	Serine protease	Exon 4	Probably damaging	Deleterious	Disease causing	Absence	Absence	Confirmed
F5	c.856 T > G	p.Phe286Val*	Serine protease	Exon 4	Possibly damaging	Tolerated	Disease causing	Absence	Absence	Confirmed
F6	c.973-1 G > A	p.(Tyr325_ Leu335del)*	Serine protease	Intron 4	NA[c]	NA[c]	NA[c]	Absence	Absence	Confirmed
F7	c.1348 G > C	p.Asp450His*	PDZ	Exon 9	Possibly damaging	Deleterious	Disease causing	Absence	Absence	Confirmed
F8	c.850 A > G	p.Ser284Gly*	Serine protease	Exon 4	Probably damaging	Deleterious	Disease causing	Absence	Absence	Confirmed
F39	c.59 C > T	p.Ala20Val	-	Exon 1	Benign	Tolerated	Polymorphism	Absence	NA[d]	Confirmed
F78	c.59 C > T	p.Ala20Val	-	Exon 1	Benign	Tolerated	Polymorphism	Absence	NA[d]	Confirmed
F133	c.367 G > T	p.Ala123Ser*	Kazal-type	Exon 1	Possibly damaging	Tolerated	Disease causing	Absence	NA[d]	Confirmed
F134	c.397 C > G	p.Arg133Gly*	Kazal-type	Exon 1	Possibly damaging	Tolerated	Disease causing	Absence	NA[d]	Confirmed
F167	c.152 A > G	p.Glu51Gly	IGFBP-like	Exon 1	Benign	Tolerated	Polymorphism	Absence	NA[d]	Confirmed
F186	c.361 A > C	p.Ser121Arg*	Kazal-type	Exon 1	Probably damaging	Deleterious	Disease causing	Absence	NA[d]	Confirmed

*Candidate variants predicted to be damaging by at least two pathogenicity prediction softwares, or affecting splicing sites.
[a]PolyPhen-2 (HumVar) / SIFT / Mutation Taster: predicted pathogenicity using these three programs.
[b]Absence: absence from the 1000 Genomes database (version 2014) or Exome Variant Server (ESP6500v2).
[c]NA: not analysed because splice variants cannot be analysed with those prediction tools.
[d]NA: not analysed because exon 1 was not covered in EVS exome database.

phenotype in Family F1. The *HTRA1* variant (c.497G > T, p.Arg166Leu) was predicted to be pathogenic by all three *in silico* prediction tools (PolyPhen-2, SIFT and MutationTaster) (Table 1). The *TTBK2* variant (c.1100A > T, p.Lys367Ile) was considered benign by PolyPhen-2, and the other three variants, located in *C15orf43* (c.307A > C, p.Ser103Arg), *CPEB1* (c.699G > C, p.Met233Ile), and *ZNF785* (c.1011C > G, p.Ser337Arg) were considered benign by at least two prediction tools.

Heterozygous *HTRA1* variants are associated with familial cerebral SVD

To test the relevance of the five candidate genes (*HTRA1*, *TTBK2*, *C15orf43*, *CPEB1*, *ZNF785*) in additional patients with SVD, multiplex Fluidigm PCR amplification of exonic regions of these genes followed by massive parallel sequencing was conducted in 191 unrelated patients with familial SVD and in Patient F1-9, used as a positive control. In addition, mutations of these five genes were searched for in whole exome sequencing data of 10 additional unrelated familial SVD probands. Eighteen exonic and/or splice site rare candidate variants were identified in 17 unrelated patients of the cohort. Fourteen of those heterozygous variants were located in *HTRA1*. Each of the four remaining variants, located in the four remaining genes, was identified in only one patient. They were all excluded based on either their prevalence in control genomic databases, or their predicted benignity by at least two *in silico* prediction tools or their occurrence in a proband showing a deleterious *HTRA1* variant (Supplementary Table 3).

Sanger sequencing was then used to confirm the presence of candidate *HTRA1* variants in all mutated probands. In addition, Sanger sequencing of *HTRA1* exon 1 and part of exons 2 and 4 was performed in all 201 probands as Fluidigm coverage of these exons was not complete. Thirteen heterozygous *HTRA1* variants were confirmed in 14 distinct probands, including F1 proband (Table 1, Fig. 3 and Supplementary Fig. 2). Eleven of these variants, including R166L (the variant identified in Family F1), were considered to be most likely deleterious. Ten of them were missense variants that were (i) absent from all interrogated databases (1000 Genomes, EVS, and IntegraGen exome databases) and from a cohort of 96 French healthy control individuals; (ii) predicted to be pathogenic by at least two *in silico* prediction tools; and (iii) affecting highly conserved amino acids (Supplementary Fig. 3). The remaining one was a splice site variant (c.973-1 G > A) absent from all databases and predicted to lead to an abnormal splicing of

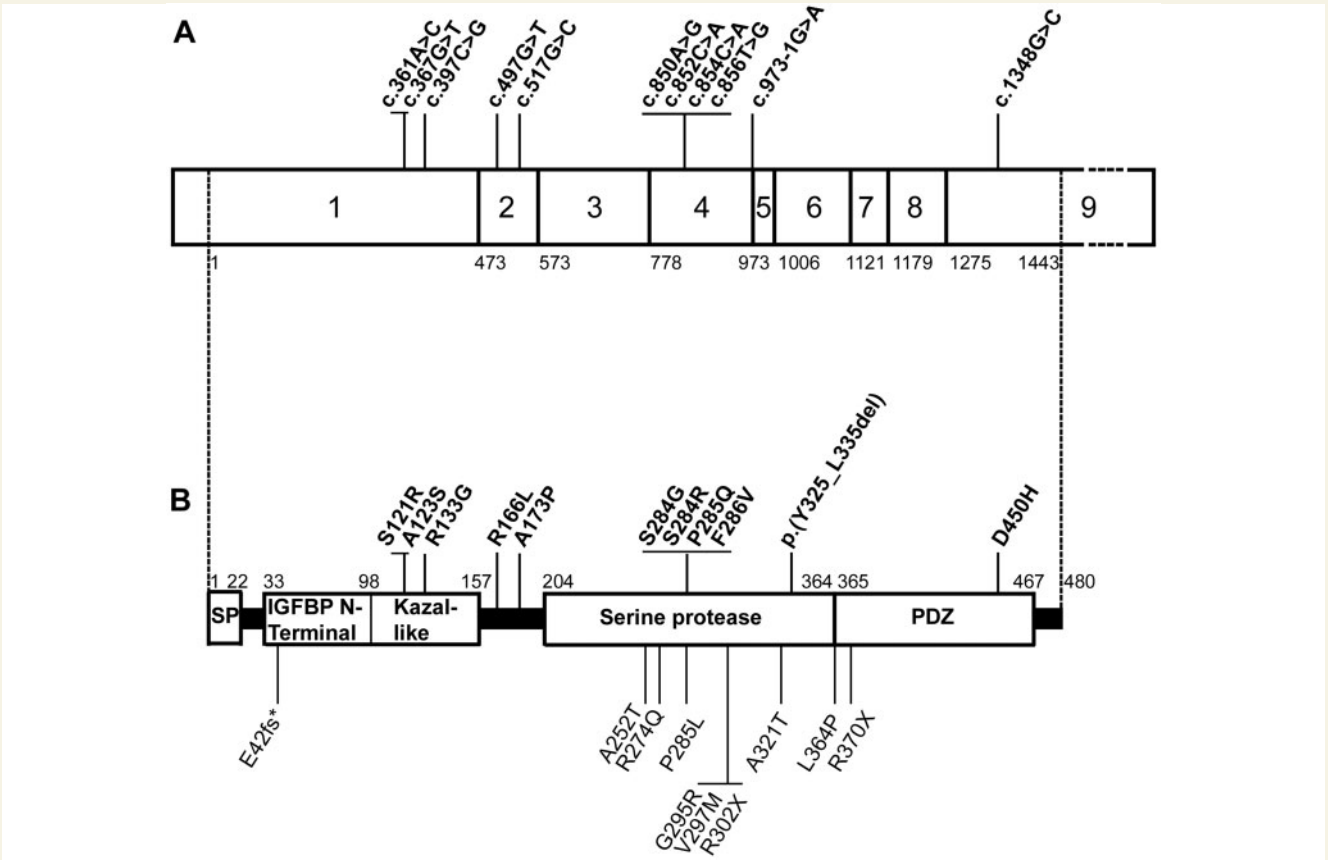

Figure 3 Schematic representation of *HTRA1* gene/protein and location of mutations. (**A**) cDNA structure of human *HTRA1* transcript NM_002775.4. Positions are annotated from the first coding nucleotide. Positions of heterozygous SVD mutations identified in this study are indicated above the figure. Numbers represent the first coding nucleotide of each exon, and the last coding nucleotide (nt 1443). (**B**) Domain organization of human HTRA1 protein (protein NP_002766.1). Above, positions of HTRA1 protein changes identified in patients with SVD in this study. Below, mutations that have been previously reported in CARASIL patients. SP = signal peptide; PDZ = PDZ-like domain. Numbers above the figure represent the first and last coding amino acids for each one of the protein domains, and the last coding amino acid (aa 480).

exon 5. This abnormally spliced mRNA would skip 33 codons including codon 328, which encodes for a serine residue required for *HTRA1* activity. The last two variants, p.Ala20Val (shared by two unrelated patients) and p.Glu51Gly, located in exon 1, were absent from databases and from our French control group but were predicted to be benign with all three prediction tools. They were not considered further. Altogether, 11 unique, and heterozygous *HTRA1* variants, including Family F1 variant, were considered as deleterious (Fig. 3).

The genealogical trees of these 11 unrelated mutated carriers are shown in Fig. 1. Family history was consistent with an autosomal dominant pattern of inheritance for at least eight of these families. Three additional affected relatives were available for Sanger sequencing in Families F5 and F8; all three were shown to be mutation carriers.

The frequency of deleterious variants was compared between our cases and control samples from two online databases: European American controls from EVS ($n = 4300$) and European controls from 1000 Genomes project ($n = 379$). All nine exons of *HTRA1* have been sequenced by the 1000 Genomes consortium whereas only eight exons (exons 2 to 9) have been sequenced in EVS. Ten likely deleterious variants located in exons 2–9 have been identified in the 4300 European American controls from EVS (one splice site change, two nonsense, and seven missense variants), as compared to seven exons 2–9 variants in our panel of 201 patients with SVD ($P = 4.2 \times 10^{-6}$; OR = 15.4; 95% CI 4.9–45.5). There is no deleterious variant in any of the *HTRA1* exons 1–9 in the 379 European controls from 1000 Genome project as compared to a total number of 10 variants in our panel of patients with SVD ($P = 2.1 \times 10^{-5}$).

Functional characterization of *HTRA1* mutations

HTRA1 encodes a conserved serine protease consisting of several domains (Fig. 3) (Clausen *et al.*, 2002). Most of the previously identified homozygous *HTRA1* mutations have been demonstrated to strongly reduce proteolytic activity

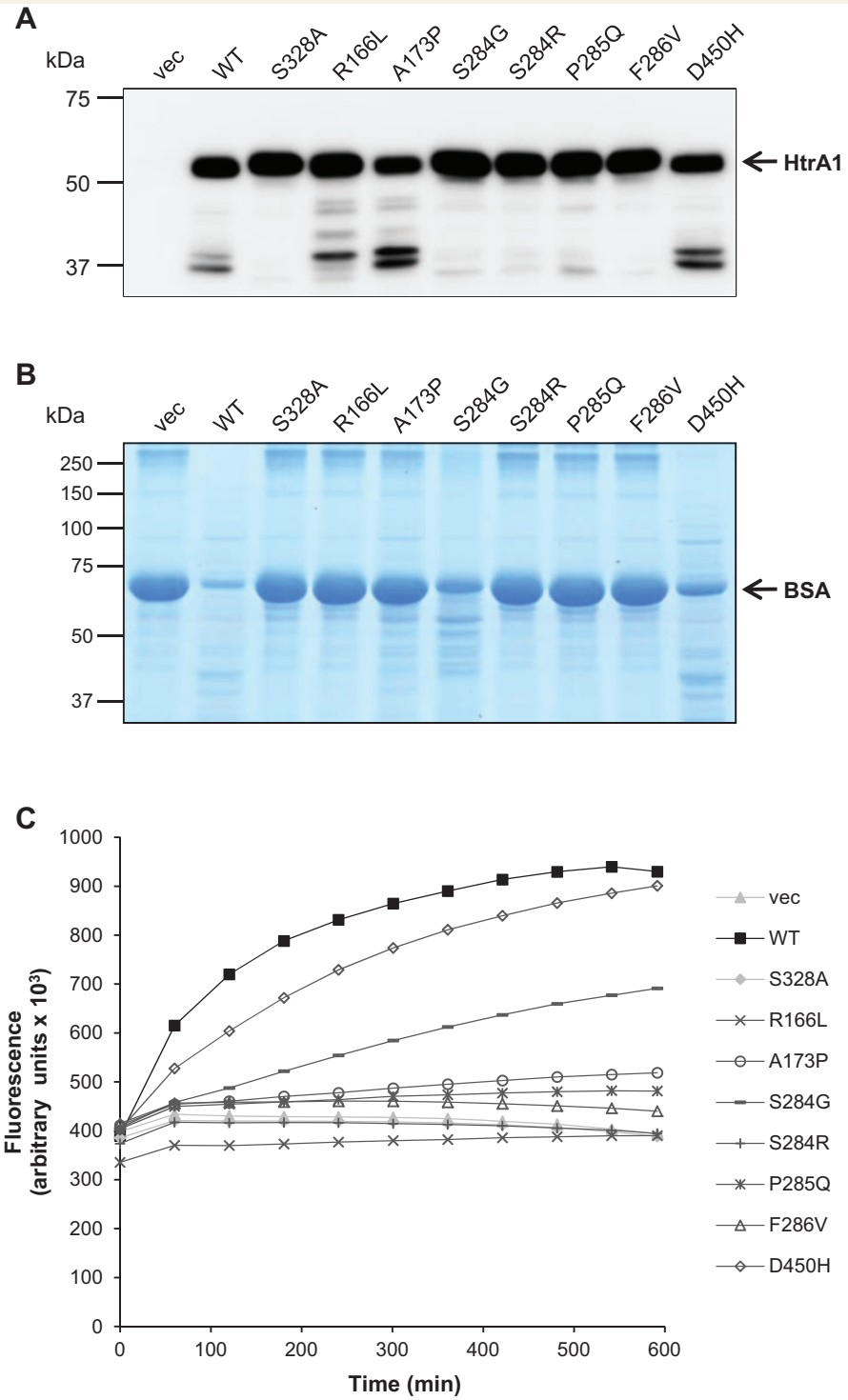

Figure 4 Most heterozygous HTRA1 mutants are proteolytically inactive. (**A**) Mutants are efficiently expressed and secreted. Upon transient transfection in HEK293T cells, anti-myc immunoblotting was performed on conditioned supernatants. Full-length HTRA1 migrates at ~55 kDa, lower molecular weight bands represent degradation products. (**B**) Proteolytic activity of conditioned supernatants was analysed towards denatured BSA and evaluated by SDS-PAGE and Coomassie Blue staining. (**C**) Proteolytic activity of conditioned supernatants was analysed towards fluorescently labeled casein over 10 h by measuring FRET. vec = vector; WT = wild-type.

(Nozaki, 2014). We therefore assessed the catalytic capacity of a subset of our heterozygous variants *in vitro* using conditioned supernatants of transiently transfected HEK 293T cells and two different substrates [bovine serum albumin (BSA) and fluorescently labelled casein]. Wild-type HTRA1 and the active-site mutant S328A were used as controls. Western blotting of cell culture media revealed efficient expression and secretion of all mutants except

Table 2 Main clinical and neuroimaging features of the 11 probands carrying deleterious heterozygous *HTRA1* mutations

	F1 R166L	F2 A173P	F3 S284R	F4 P285Q	F5 F286V	F6 c.973-1G > A	F7 D450H	F8 S284G	F133 A123S	F134 R133G	F186 S121R
Sex	Male	Female	Female	Male	Male	Female	Male	Female	Male	Female	Male
Age at onset (years)	66	65	-	50	49	66	68	62	-	-	56
Age at time of study (years)	69	72	49	55	55	66	72	62	50	58	66
No. of affected relatives[a]	4	1	2	1	1	1	1	2	4	1	3
Hypertension	No	Yes	Yes	No	No	Yes	Yes	No	Yes	No	No
Symptoms at disease onset (or symptoms that led to MRI)[b]	Cognitive decline	Balance impairment	(Headaches)	Stroke	Stroke	Stroke	TIA	Stroke	(Seizures)	(Headaches)	Balance impairment
History of TIA or ischaemic stroke	Yes	No	No	Yes	Yes	Yes	Yes	Yes	No	No	No
Cognitive impairment	Yes	Yes	No	No	Yes	N.A.	Yes	No	No	No	Yes
Dementia	No	No	No	No	No	No	No	No	No	No	Yes
Gait disturbance	Yes	Yes	No	Yes	Yes	N.A.	Yes	No	No	No	Yes
MRI features											
Age at MRI (years)	69	72	49	50	55	66	70	62	50	58	62
WMH	Yes	Yes	Yes	Yes	Yes	Yes	Yes	Yes	Yes	Yes	Yes
early confluent	-	-	-	Yes	-	-	-	-	Yes	Yes	Yes
confluent	Yes	Yes	Yes	-	Yes	Yes	Yes	Yes	-	-	-
Status cribrosum[c]	Yes	Yes	N.A.	Yes	N.A.	Yes	N.A.	Yes	Yes	No	Yes
Lacunes	Yes	Yes	Yes	Yes	Yes	Yes	Yes	Yes	Yes	No	Yes
Microbleeds[d]	No	N.A.	No	N.A.	N.A.	Yes	N.A.	Yes	No	N.A.	No

[a]Affected relatives, based on family history and/or clinical charts (see Fig. 1).
[b]Symptoms which led to MRI are possibly not related to the disease.
[c]The presence of 'status cribrosum' was evaluated when T_2 sequence or/and T_1 sequence with thin-slice were available.
[d]The presence of microbleeds was evaluated when gradient-echo sequences were available.
N.A. = not available; TIA = transient ischaemic attack; WMH = white matter hyperintensties.

for A173P and D450H, which were present at somewhat reduced levels, possibly due to increased autodegradation (Fig. 4A). In the BSA assay *HTRA1* mutants R166L, A173P, S284R, P285Q and F286V showed a loss of activity comparable to the S328A mutant (Fig. 4B). In contrast, the reduction observed for S284G and D450H was only partial. These results were fully confirmed using casein as substrate in a Fluorescent Resonance Energy Transfer (FRET) assay yielding a fluorescence increase upon casein degradation (Fig. 4C). While D450H and S284G displayed residual activity, all other mutants showed a behaviour similar to the loss-of-function controls.

Main clinical features of the unrelated probands with heterozygous *HTRA1* mutations

Main clinical and MRI features of the 11 unrelated probands with *HTRA1* heterozygous mutations are summarized in Table 2, Figs 2, 5 and Supplementary Fig. 4. Genealogical trees are shown in Fig. 1. The clinical picture is characterized by the association of subcortical ischaemic events and cognitive decline starting in most patients in the sixth decade. None of these patients had early-onset alopecia or early-onset spondylosis. Three of them (Patients F1-9, F3 and F6 index) suffered from a lumbar disk prolapse but late in life. Typical neuroimaging findings include confluent or early confluent white matter hyperintensities on MRI T_2-weighted and FLAIR images, with frequent involvement of the external and internal capsules, sometimes associated with multiple lacunar infarcts and microbleeds (Figs 2, 5 and Supplementary Fig. 4). Anterior temporal regions and U fibres were spared. Dilated perivascular spaces with a typical 'status cribrosum' characterized by an innumerable number of dilated Virchow-Robin spaces and resulting in a cribriform change in basal ganglia were observed in most patients. Altogether, the clinical and MRI features of these *HTRA1* heterozygous patients are similar to the ones of sporadic SVD cases.

Discussion

We report herein a family including three affected individuals with a cerebral SVD of previously unknown aetiology, which segregates as an autosomal dominant disorder. Linkage analysis in combination with whole exome sequencing performed in this family (F1) as well as high throughput sequencing in a panel of 201 unrelated familial SVD cases (in whom *NOTCH3* mutations were previously

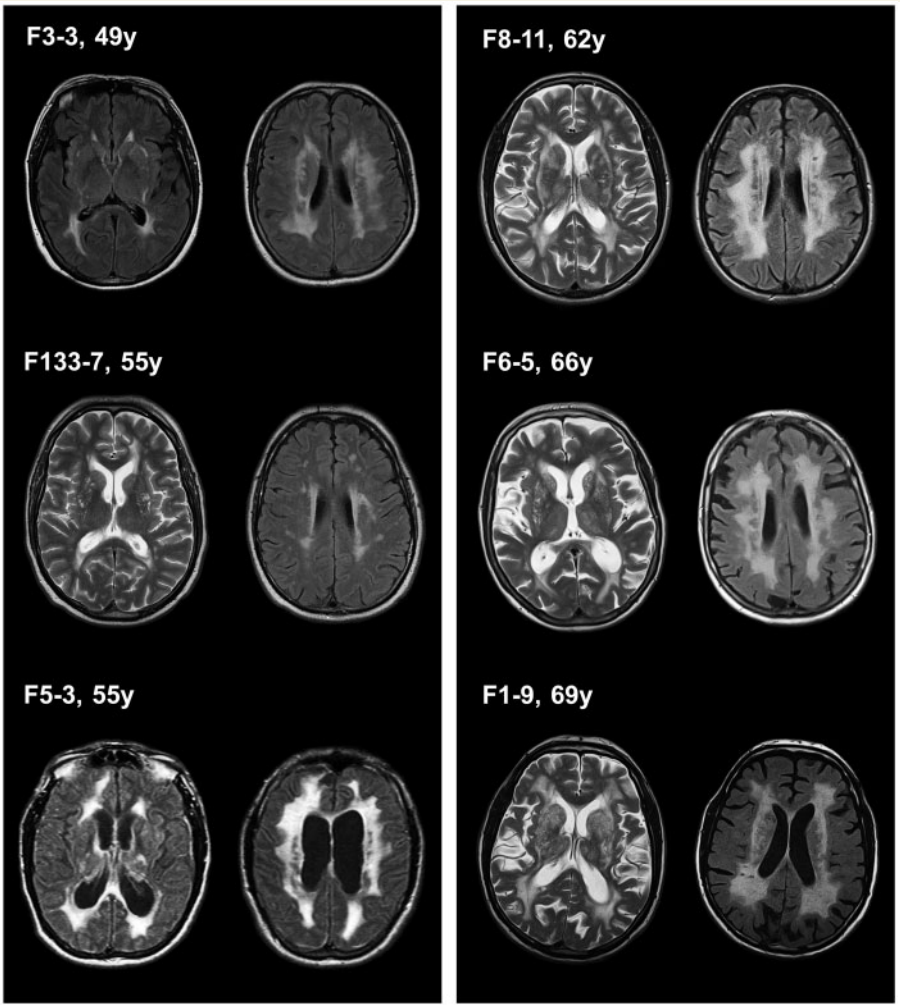

Figure 5 Status cribrosum and white matter hyperintensity characteristics in *HTRA1* mutated probands. Status cribrosum is well visible on T_2-weighted images in Patients F133-7, F8-11, F6-5, and F1-9. white matter hyperintensitiess on FLAIR images were extensive in all cases after 60 years of age. Some of the younger patients had more limited white matter hyperintensities, such as Patient F133-7.

excluded) strongly suggest that (i) the causative mutation in Family F1 is a heterozygous mutation located in *HTRA1*; and (ii) roughly 5% of familial SVD of unknown aetiology are associated with heterozygous *HTRA1* mutations.

Clinical features of this autosomal dominant SVD differ from those of CARASIL by a later age at onset of stroke and cognitive decline (20–30 years in age at onset) and the absence of the typical CARASIL extra-neurological symptoms (Maeda *et al.*, 1976; Nozaki *et al.*, 2014). Indeed, none of our patients presented with early-onset alopecia or early-onset spondylosis. Three of them were reported to have osteoporosis and lumbago, but those manifestations occurred late in life. The phenotype of this condition is very close to those observed in sporadic SVD cases. Indeed, the occurence of lacunar ischaemic events between 55 and 72 years in half of the cases and the progressive gait disturbance and subcortical cognitive impairment from the age of 60 are comparable with the phenotype of age and hypertension related SVD. The MRI pattern is also very similar except for the presence of a status cribrosum, which seems to be more frequent in this condition, and for the location of microbleeds which involves preferentially the deep and juxtacortical hemispheric areas.

Several observations strongly support the pathogenic role of the heterozygous *HTRA1* mutations in the 11 probands reported herein. First, all these mutations are absent from the 1000 Genomes ($n = 379$ Europeans) and EVS databases as well as from our panel of French controls. Second, there is a highly significant difference between the frequency of deleterious *HTRA1* variants in our panel of familial SVD probands and that in control databases, including the EVS database ($n = 4300$ European-Americans; $P = 4.2 \times 10^{-6}$; OR = 15.4; 95% CI 4.9–45.5) and 1000 Genomes database ($n = 379$ Europeans; $P = 2.1 \times 10^{-5}$). Third, all 11 mutations are predicted to be deleterious by at least two *in silico* prediction tools. Fourth, a complete loss of activity was observed for five of the seven variants tested. An additional variant located in a consensus splice site (c.973-1G > A), is predicted to lead to an in-frame deletion of exon 5, which

includes the codon 328 encoding a serine required for enzyme activity; this variant is also most likely a loss-of-function mutant. The residual activity of the variants S284G and D450H might be the result of a pathomechanism different from intrinsic proteolytic activity alteration such as protein destabilization or mislocalization. In any case, both our genetic data and the results of *in silico* prediction tools analyses strongly argue for their pathogenic potential. Additional work on large series of patients is required to elucidate how these mutants might alter HTRA1 function.

The most surprising finding of this study is the deleterious role of heterozygous mutations in *HTRA1*, a gene previously reported to be involved in a very rare autosomal recessive SVD (Hara *et al.*, 2009). Indeed, CARASIL was initially reported in siblings from a consanguineous family with unaffected parents. So far 12 mutated CARASIL families have been reported, including 10 consanguineous families (Nozaki *et al.*, 2014). The largest series includes six families from Japan; all of these were consanguineous families and parents of affected cases were reported as being unaffected (Hara *et al.*, 2009). Half of these families harboured homozygous stop codons. Unaffected parents were further mentioned in two other consanguineous families from Japan and Turkey (Nishimoto *et al.*, 2011; Bayrakli *et al.*, 2012). Interestingly, however, in three additional families, cerebral MRI performed in either one or both parents was reported to show a leukoencephalopathy, raising the question of the causality of the heterozygous variants carried by these parents; in the last family, both parents were said to be deceased in their fifties with emotional liability, but MRI was not available (Mendioroz *et al.*, 2010; Wang *et al.*, 2012; Chen *et al.*, 2013; Bianchi *et al.*, 2014). None of our families is consanguineous and 8 of 11 of them show a pattern of inheritance consistent with autosomal dominant inheritance. Altogether, these data strongly suggest that in some cases *HTRA1* mutations behave as autosomal recessive mutations, with heterozygous carriers being clinically unaffected, as observed in Japanese CARASIL patients. In other cases, *HTRA1* mutations behave as dominant mutations, with heterozygous carriers being clinically affected; based on our data, their frequency is predicted to be much higher than recessive type mutations. One of our current hypotheses to reconcile those data is that some of the missense mutations reported herein might be dominant negative mutations, the mutated allele being a loss of function mutant which interferes with the normal function of the remaining wild-type allele, leading to a further decrease in enzyme activity. In contrast, mutations leading to premature stop codons would lead to the decay of the mutated mRNA, the absence of synthesis of the protein encoded by the mutated allele and therefore to a haploinsufficiency which by itself would not be sufficient to cause SVD. This has been reported in several other diseases, such as hypertension caused by *KLHL3* mutations or myopathies associated with *COL6A1* mutations (Boyden *et al.*, 2012; Zou *et al.*, 2014). Interestingly, in most of these diseases that exist both as dominant and recessive disorders, the causative gene encodes proteins acting as dimers or multimers. *HTRA1* encodes a serine protease whose functional unit is a trimer stabilized by residues of the protease domain (Clausen *et al.*, 2002). Another non-mutually exclusive hypothesis would be that some of these missense mutations are semi-dominant mutations. Comparative measurement of the residual HTRA1 endogenous activity of fibroblasts from missense and stop codons heterozygous carriers would be needed to investigate further this question but this test is not currently available. Our last hypothesis would be that in some CARASIL families the affected status of the heterozygous parents would have been overlooked due to the much later age at onset in heterozygous carriers as compared to offsprings with biallelic mutations; indeed, there is roughly 20–30 years difference in age at onset between heterozygous and biallelic mutated patients.

The identification of the causative gene in these families now allows molecular genetic screening for this condition. Knowing that the clinical and MRI features of the patients reported herein were similar to those observed in sporadic SVD cases except for the familial nature of the disease, molecular screening of *HTRA1* would be indicated in all cases with a familial SVD, in the absence of clinical or MRI findings suggestive of another condition. However, the familial nature of the disease may be overlooked due to the late onset of clinical symptoms. Therefore, molecular screening should be considered in sporadic cases when the extent of microvascular lesions on MRI contrasts with the paucity of vascular risk factors.

In summary, we show herein that nearly 5% of familial SVDs referred for molecular screening are associated with deleterious heterozygous mutations of *HTRA1*. Therefore, these mutations would be so far the second cause of autosomal dominant SVD after CADASIL. This autosomal dominant SVD is characterized by a much later age of onset than in CARASIL and the absence of typical extra-neurological CARASIL features. Further assessment of pathogenic molecular effects of those heterozygous variants and delineation of the complete mutation spectrum will now be needed to develop efficient genetic diagnosis.

Acknowledgements

We thank all families for their participation in this study. We are also indebted to F. Marchelli for excellent figures editing.

Funding

The research was funded by INSERM, Programme Hospitalier de Recherche Clinique AOM06037 (grant to E.T.L.), Leducq Foundation 2007 grant 'Identification of

novel targets for hemorrhagic stroke' (grant to E.T.L.), the Leducq transatlantic network 'Pathogenesis of Small Vessel Disease of the Brain' (grant to M.D.), the Vascular Dementia Research Foundation and the Deutsche Forschungsgemeinschaft (DFG).

Supplementary material

Supplementary material is available at *Brain* online.

References

Bayrakli F, Balaban H, Gurelik M, Hizmetli S, Topaktas S. Mutation in HTRA1 gene in a patient with degenerated spine as a component of CARASIL syndrome. Turkish Neurosurg 2012; 24: 67–9.

Beaufort N, Scharrer E, Kremmer E, Lux V, Ehrmann M, Hubert R, et al. Cerebral small vessel disease-related protease Htra1 processes latent TGF-β binding protein 1 and facilitates TGF-β signaling. Proc Natl Acad Sci USA 2014; 111: 16496–501.

Bianchi S, Di Palma C, Gallus GN, Taglia I, Poggiani A, Rosini F, et al. Two novel HTRA1 mutations in a European CARASIL patient. Neurology 2014; 82: 898–900.

Boyden LM, Choi M, Choate KA, Nelson-Williams CJ, Farhi A, Toka HR, et al. Mutations in Kelch-like 3 and cullin 3 cause hypertension and electrolyte abnormalities. Nature 2012; 482: 98–102.

Chabriat H, Joutel A, Dichgans M, Tournier-Lasserve E, Bousser MG. Cadasil [Review]. Lancet Neurol 2009; 8: 643–53.

Chen Y, He Z, Meng S, Li L, Yang H, Zhang X. A novel mutation of the high-temperature requirement A serine peptidase 1 (HTRA1) gene in a Chinese family with cerebral autosomal recessive arteriopathy with subcortical infarcts and leukoencephalopathy (CARASIL). J Int Med Res 2013; 41: 1445–55.

Clausen T, Southan C, Ehrmann M. The HTRA family of proteases: implications for protein composition and cell fate. Mol Cell 2002; 10: 443–55.

Gould DB, Phalan FC, van Mil SE, Sundberg JP, Vahedi K, Massin P, et al. Role of COL4A1 in small-vessel disease and hemorrhagic stroke. N Engl J Med 2006; 354: 1489–96.

Hara K, Shiga A, Fukutake T, Nozaki H, Miyashita A, Yokoseki A, et al. Association of HTRA1 mutations and familial ischemic cerebral small-vessel disease. N Engl J Med 2009; 360: 1729–39.

Joutel A, Corpechot C, Ducros A, Vahedi K, Chabriat H, Mouton P, et al. Notch3 mutations in CADASIL, a hereditary adult-onset condition causing stroke and dementia. Nature 1996; 383: 707–10.

Mendioroz M, Fernandez-Cadenas I, Del Rio-Espinola A, Rovira A, Solé E, Fernandez-Figueras MT, et al. A missense HTRA1 mutation expands CARASIL syndrome to the Caucasian population. Neurology 2010; 75: 2033–5.

Maeda S, Nakayama H, Isaka K, Aihara Y, Nemoto S. Familial unusual encephalopathy of Binswanger's type without hypertension. Folia Psychiatr Neurol Jpn 1976; 30: 165–77.

Nishimoto Y, Shibata M, Nihonmatsu M, Nozaki H, Shiga A, Shirata A. A novel mutation in the HTRA1 gene causes CARASIL without alopecia. Neurology 2011; 76: 1353–5.

Nozaki H, Nishizawa M, Onodera O. Features of cerebral autosomal recessive arteriopathy with subcortical infarcts and leukoencephalopathy. Stroke 2014; 45: 3447–53.

Pantoni L. Cerebral small vessel disease: from pathogenesis to clinical characteristics to therapeutic challenges. Lancet Neurol 2010; 9: 689–701.

Revesz T, Holton JL, Lashley T, Plant G, Frangione B, Rostagno A, et al. Genetics and molecular pathogenesis of sporadic and hereditary cerebral amyloid angiopathies. Acta Neuropathol 2009; 118: 115–30.

Wang XL, Li CF, Guo HW, Cao BZ. A Novel mutation in the HTRA1 gene identified in Chinese CARASIL pedigree. CNS Neurosc Ther 2012; 18: 867–9.

Wardlaw JM, Smith C, Dichgans M. Mechanisms of sporadic cerebral small vessel disease: insights from neuroimaging. Lancet Neurol 2013; 12: 483–97.

Zou Y, Zwolanek D, Izu Y, Ganhdy S, Schreiber G, Brockmann K, et al. Recessive and dominant mutations in COL12A1 cause a novel EDS/myopathy overlap syndrome in humans and mice. Hum Mol Genet 2014; 23: 2339–52.